NANO LETTERS

2007
Vol. 7, No. 11
3383−3387

Dynamics of Strongly Degenerate Electron–Hole Plasmas and Excitons in Single InP Nanowires

Lyubov V. Titova,[†] Thang Ba Hoang,[†,‡] Jan M. Yarrison-Rice,[§] Howard E. Jackson,[†] Yong Kim,[∥,⊥] Hannah J. Joyce,[⊥] Qiang Gao,[⊥] H. Hoe Tan,[⊥] Chennupati Jagadish,[⊥] Xin Zhang,[#] Jin Zou,[#] and Leigh M. Smith*

Department of Physics, University of Cincinnati, Cincinnati, Ohio 45221-0011, Department of Physics, Miami University, Oxford, Ohio 45056, Department of Electronic Materials Engineering, Research School of Physical Sciences and Engineering, Australian National University, Canberra ACT 0200, Australia, Department of Physics, College of Natural Science, Dong-A University, Hadan 840, Sahagu, Busan 604-714, Korea, and School of Engineering and Centre for Microscopy and Microanalysis, University of Queensland, St. Lucia, OLD 4072, Australia

Received July 18, 2007; Revised Manuscript Received September 12, 2007

ABSTRACT

Low-temperature time-resolved photoluminescence spectroscopy is used to probe the dynamics of photoexcited carriers in single InP nanowires. At early times after pulsed excitation, the photoluminescence line shape displays a characteristic broadening, consistent with emission from a degenerate, high-density electron–hole plasma. As the electron–hole plasma cools and the carrier density decreases, the emission rapidly converges toward a relatively narrow band consistent with free exciton emission from the InP nanowire. The free excitons in these single InP nanowires exhibit recombination lifetimes closely approaching that measured in a high-quality epilayer, suggesting that in these InP nanowires, electrons and holes are relatively insensitive to surface states. This results in higher quantum efficiencies than other single-nanowire systems as well as significant state-filling and band gap renormalization, which is observed at high electron–hole carrier densities.

Semiconductor nanowires have been successfully incorporated into a variety of nanoscale devices as both active elements[1−10] and device interconnects.[5,11−13] However, important questions remain about the optical properties of these structures, particularly concerning photoexcited carrier dynamics and relaxation, which are crucial for the design optimization and ultimately the success of nanowire-based optical devices. Moreover, because such nanowires are not small on a quantum level, they can support excitation of a degenerate density of electrons and holes, so that many-body effects can be quite prominent.

In this letter, we use low-temperature time-resolved photoluminescence (TRPL) spectroscopy to probe the dynamics of electrons and holes in single InP nanowires. As we will show, electrons and holes in InP are particularly insensitive to surface states, which cause extremely short recombination lifetimes and low quantum efficiencies in other nanowire systems including CdS, GaAs, and GaAs/GaAlAs.[14−19] The surface recombination velocity, S, one metric often used to characterize the effect of nonradiative surface (or interface) states, is notably different in different semiconductors. The surface recombination velocity in as-grown, undoped epilayers in InP is $S \sim 10^3$ cm/s,[20,21] while GaAs exhibits velocities nearly a 1000 times higher: $S \sim 10^6$ cm/s.[22,23] Such a difference should have a dramatic impact on the nonradiative lifetime in nanowires. Thus equivalent 40 nm diameter GaAs or InP nanowires should exhibit nonradiative lifetimes ($\tau_{nr} \sim d/2S$) differing by a factor of 1000, from 4 ps in GaAs to 4 ns in InP.[23] This is consistent with our previous measurements of the recombination lifetimes in single GaAs nanowires and GaAs/AlGaAs core−shell nanowires, which were found to be less than 50 ps, limited by the system time response.[14,16] Parkinson et al. used THz pump−probe measurements in an ensemble of bare GaAs nanowires to extract a 270 fs carrier lifetime at 300 K.[24] We therefore expect InP nanowires to exhibit significantly higher quantum efficiencies, which will allow us to

* Corresponding author. E-mail: leigh.smith@uc.edu.
[†] Department of Physics, University of Cincinnati.
[‡] On leave from Institute of Materials Science, VAST, Hanoi, Vietnam.
[§] Department of Physics, Miami University.
[∥] Department of Physics, Dong-A University.
[⊥] Department of Electronic Materials Engineering, Australian National University.
[#] School of Engineering and Centre for Microscopy and Microanalysis, the University of Queensland.

10.1021/nl071733l CCC: $37.00
Published on Web 09/29/2007

measure the intrinsic exciton lifetime in single nanowires as well as to enable us to probe many-body interactions at high electron−hole carrier densities.

Unlike the case of state filling in quantum dots and related quantum-confined systems where the density of states is discrete along at least one or more dimensions, the nanowires studied here have diameters significantly larger than the exciton Bohr radius, and therefore no quantum confinement effects are expected. Under high excitation density conditions, emission from an electron−hole plasma (EHP) should be observed with Fermi energies that show significant occupation at higher energies at early times. One characteristic signature of such large electron−hole carrier densities are many-body interactions, which induce a renormalization of the band gap. The band gap renormalizes, moving to lower energies as a result of the increased exchange and correlation energy of the carriers. Using a theoretical estimate of the band gap renormalization (BGR), we will show self-consistently that, for the measured EHP spectra, the BGR scales with the increased Fermi energy expected for an EHP of a particular density.

InP nanowires were grown on a (111)B-oriented InP substrate by 30 nm gold catalyst-assisted MOCVD at a temperature of 420 °C, with V/III molar ratio of 110. Individual nanowires were removed from the growth substrate into a dilute methanol solution and deposited onto either a silicon substrate (for optical measurements) or holey carbon film (for transmission electron microscopy (TEM) measurements). For comparison, a 5 μm thick epilayer was grown in the same reactor on a (100)-oriented InP substrate at a temperature of 420 °C. For TRPL, as well as for the time-integrated PL measurements, single nanowires (or the thick epilayer) were excited with 780 nm (1.58 eV), 200 fs pulses at a repetition rate of 76 MHz at an average power of 3 mW focused to a 2 μm spot on the nanowire. Time-integrated PL spectra were recorded with a thermoelectrically cooled CCD detector, while the TRPL measurements were performed using a silicon avalanche photodiode in combination with time-correlated single-photon counting with 80 ps resolution. All measurements were carried out at 10 K.

TEM investigations were carried out in a Philips F20 TEM operating at 200 keV. Figure 1a shows a bright-field TEM image of a selected single InP NW. The 7 μm long InP nanowire is approximately 80 nm in diameter and tapers to 30 nm at the tip of the NW. Figure 1b shows a high-magnification TEM image of the tip with the 30 nm gold catalyst clearly visible. Figure 1c shows a selected area electron diffraction pattern of the ⟨111⟩ zone axis, confirming that the NW has the ZB structure with the growth direction of [$\bar{1}\bar{1}\bar{1}$]. SEM images (not shown) of similar NWs dispersed onto silicon substrates showed the majority of InP NWs were ∼2 μm long with diameters ranging from 80 to 100 nm. The large majority of dispersed NWs do not show an intact Au catalyst particle, probably because of the sonication process.

We have investigated 15 single nanowires and found that their emission spectra consist of broad (fwhm 30−80 meV) near band edge emission peaks with energy varying from

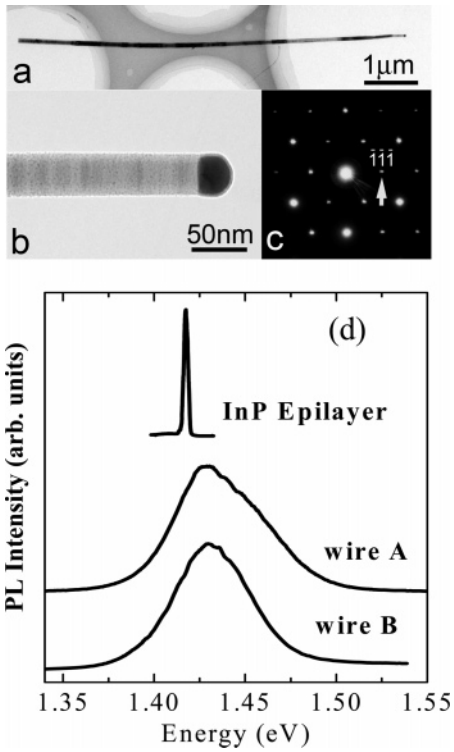

Figure 1. (a) Bright-field TEM image of selected InP nanowire. (b) High-magnification image of NW tip with intact Au catalyst. (c) Selected area electron diffraction of the ⟨111⟩ zone axis, confirming the ZB structure and NW growth along [$\bar{1}\bar{1}\bar{1}$]. (d) normalized time-integrated PL spectra of two single InP nanowires, wire A and wire B, as well as an InP epilayer.

1.37 to 1.48 eV, sometimes accompanied by low- and high-energy shoulders. In addition, we have observed that the emission intensity also varies by nearly an order of magnitude. We have observed that particularly strong emission from a nanowire is correlated with emission energy centered at 1.418 eV as expected for zinc-blende InP.[25] Typical time-integrated normalized PL spectra for two such selected single InP nanowires are shown in Figure 1b along with the PL spectrum of a 5 μm thick (100)-oriented InP epilayer grown in the same reactor under optimized growth conditions for comparison. With 200 fs, 780 nm pulsed excitation, both nanowires (A and B) exhibit broad (∼60 meV) emission peaks at energies above the InP epilayer emission (1.418 eV) with nanowire A, exhibiting a high-energy shoulder. We note that the emission intensity of such selected InP nanowires is 1−2 orders of magnitude higher than that of the core−shell GaAs/AlGaAs nanowires excited under similar excitation conditions.[14,16] This enhanced quantum efficiency for InP wires is consistent with the lower susceptibility of InP nanowires to the nonradiative surface states.[19−21]

The time-integrated spectra of Figure 1d displays an average over time and so over density. The initial electron−hole densities created by the 200 fs laser pulse are quite large, and so the time-integrated spectrum Figure 1d displays an average response that is at only a slightly lower carrier density. In contrast, single-nanowire time-resolved photoluminescence (TRPL) measurements provide further insight

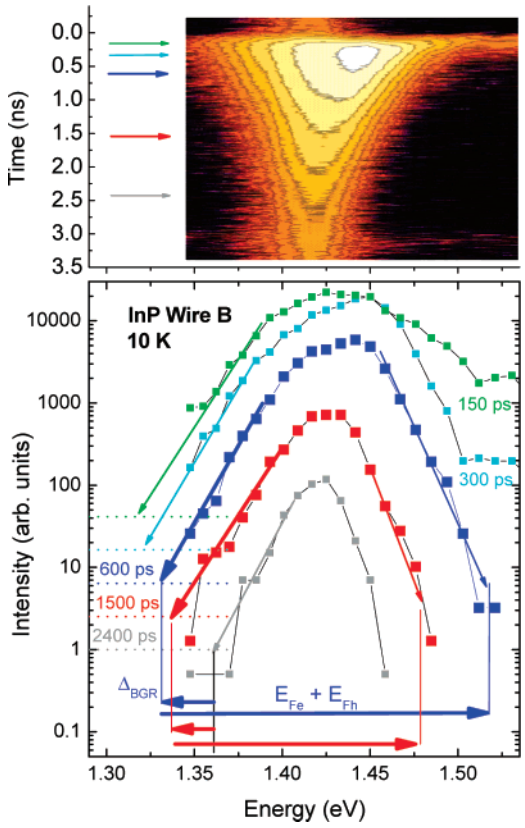

Figure 2. (a) Map of time-resolved photoluminescence spectrum of wire B. Time moves from zero at the top to 3.5 ns at the bottom of the map, and the spectral intensities are shown in log scale from 1.35 to 1.57 eV. (b) Five slices in the time evolution of the PL spectrum of wire B on a semilog plot, extracted from the TRPL map above at times designated by arrows to left of (a). Dashed lines indicate background levels. Band gap renormalization and sum of electron and hole Fermi energies are shown as colored arrows for the 600 and 1500 ps spectra.

into the nature of electronic states and exciton dynamics in these nanowires. The TRPL measurement allows one in a single experiment to follow the evolution of these carriers from very high to extremely low densities. The TRPL spectrum of wire B is shown in Figure 2a as a false-color image on a logarithmic intensity scale, with the vertical axis corresponding to the time after the laser pulse and the horizontal axis corresponding to the emission energy. At early times after the laser pulse, one observes emission at both significantly higher energies and significantly lower energies than the exciton peak at 1.418 eV. Both the higher- and lower-energy PL converge toward the exciton peak energy at later times. It is important to note that at late times (and so low electron−hole densities) the FWHM line width of the PL emission is only 20 meV and exactly centered at 1.418 eV, which is the emission energy of a free exciton in InP. This behavior is displayed in the PL spectra of wire B, shown in Figure 2b, which are PL time slices from 150 ps to 2.4 ns after the excitation pulse (note horizontal arrows in Figure 2a that indicate the particular time slices displayed in Figure 2b). The PL spectra in Figure 2b are shown on a logarithmic scale to emphasize the low- and high-energy emission seen at early times. Wire B exhibits a broad emission line with a peak at ~1.45 eV at early times, which rapidly narrows and red-shifts to 1.42 eV at later times. The electrons and holes rapidly cool so that the high-energy tail drops to background levels by ~600 ps after the laser pulse. In addition, one can see in Figure 2b emission at energies significantly below the exciton line. This low-energy PL response also decays to the background level with increasing time. Extrapolating this low-energy response, using linear fits for each time slice, allows us to define the bottom of the emission band. The straight colored lines on the left of each time slice are fits to the low-energy data points extrapolated down to the background of each spectra (denoted by the dashed lines). Spectra are offset vertically for clarity. The bottom of the emission band at 150 ps, for instance, is at 1.32 eV, approximately 40 meV below the low-energy edge of the exciton line (1.36 eV) at late times.

The time-resolved spectra from the single InP nanowire (B) shown in Figure 2b provides strong evidence for the formation of a degenerate electron−hole plasma. At early times and high electron−hole densities, excitons are completely ionized because of screening, but once the average carrier density becomes lower than the Mott density, excitons reappear. At the earliest times, 150 ps after the laser pulse, we observe that the emission response extends over 250 meV, from 1.3 to 1.55 eV. Such an energy range, from the bottom of the emission band to the top, is a measure of the sum of the electron and hole Fermi energies. The bottom of the band is below the exciton energy because of the significant effect of the increased exchange and correlation energies that occur at high densities, resulting in a band gap renormalization (BGR).[26,27] The high-energy and low-energy tails converge on the exciton line at later times because of the reduced Fermi energies and reduced BGR at lower electron and hole densities.

These dynamics are also supported by the time decays shown in Figure 3, which are extracted from the map in Figure 2a at different emission energies. At the highest energies (1.49 eV), the time decays are single exponential with an extremely short recombination lifetime of 90 ps, nearly limited by our system response for the silicon APD of 80 ps. At lower energies, the recombination time is longer, reaching 500 ps at 1.45 eV and a maximum of 1.1 ns at an energy just below the exciton recombination line at 1.418 eV. At the lowest energies, however, the decay time is also short, reflecting the density-dependent band gap renormalization (BGR). Once the carrier density decreases below the Mott density, the excitons reappear with a recombination lifetime of 1.1 ns in wire B. This lifetime is nearly equal to the recombination lifetime of 1.67 ns we observe in a 5 μm thick epilayer grown on the 100-oriented InP substrate (not shown). Wire A shows similar behavior although state filling at high energies is more prominent in this wire, resulting in TRPL spectra that exhibit a several hundred picosecond delay before a single-exponential decay is observed. Before this time, high-energy electrons continue to fill in the slightly lower excited states from above. This phenomena is seen to a lesser degree in Wire B (see the 1.42 eV spectra), where single-exponential decay is seen ~500 ps after excitation.

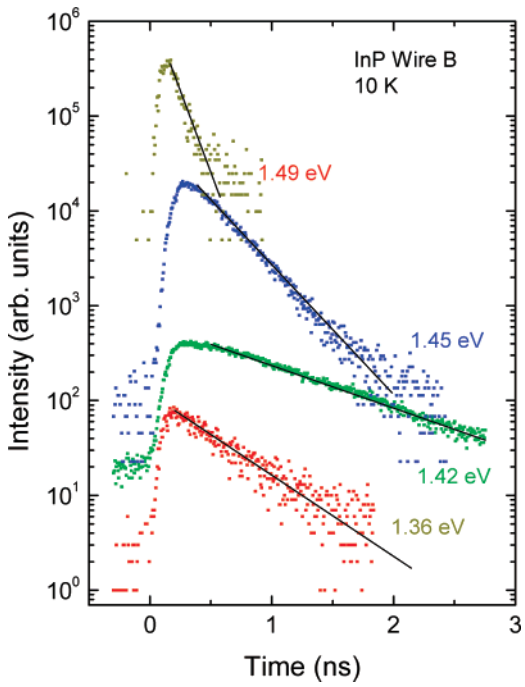

Figure 3. Photoluminescence time decays at four different energies on a semilog plot, extracted from the TRPL map shown in Figure 2a. Solid lines are fit to the exponential decays at each energy.

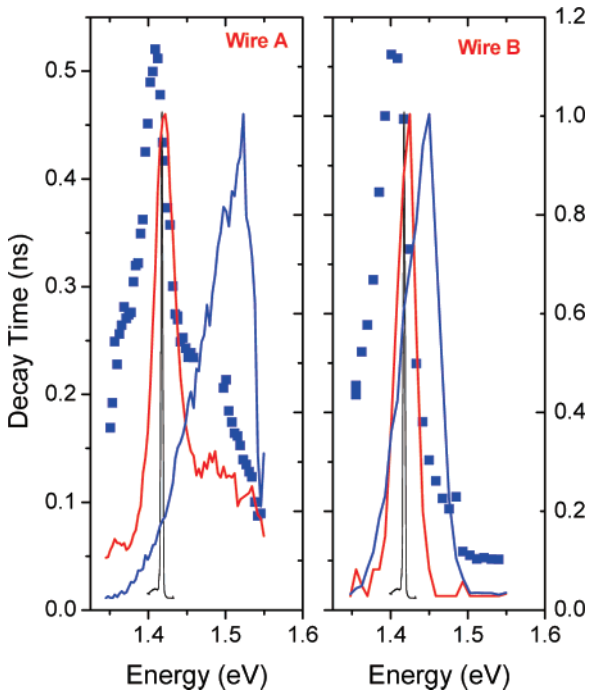

Figure 4. Recombination lifetimes at different emission energies of (a) wire A and (b) wire B shown with square points. The black narrow solid lines are the PL spectra of the InP epilayer. Blue solid PL spectra are taken at 300 ps after excitation for each NW, and red solid PL spectra are from 2.4 ns after excitation.

Considering the BGR further, recall that excitons in InP have Bohr radii of 9 nm and binding energies of 5.1 meV. The nanowires have diameters greater than 50 nm, and thus no quantum confinement effects are expected. The photoexcited carriers therefore will lie within the full three-dimensional band of electron and hole continuum states. At very low excitation densities (equivalent to the emission at late times in a time-resolved experiment), the electrons and holes predominantly exist in hydrogenic bound states called excitons. As the density of carriers increases, the binding energy decreases because of screening. Haug and Schmitt-Rink have shown that a zero-temperature estimate of the Mott density where excitons ionize should be $\sim 10^{17}$ cm^{-3}.[26] Above this density, excitons are not bound, and so only an electron hole plasma can be observed. At all densities, regardless of the degree of screening, as long as excitons are observed, they are seen to emit at the same spectral energy. As the exciton binding energy decreases, the band gap renormalizes (decreases) as well. The excitons ionize when the renormalized band gap crosses through the exciton energy level (i.e., the exciton binding energy is zero). At even higher densities, the renormalized gap continues to decrease as the electron−hole density increases.

The renormalization of the band gap occurs because of the increased exchange and correlation energies that occur at higher electron−hole densities. Although Schmitt-Rink and others have extended theoretical work on band gap renormalization to quantum systems, the qualitative behavior of 3D systems is still appropriately described by the work of Vashishta and Kalia,[26] who showed that the sum of the exchange and correlation energies are independent of the particular band structure and depend only on the relative distance between the electron−hole pairs and the exciton binding energy (ϕ_x) at low densities: $\Delta_{BGR} = \phi_x(-4.8316 - 5.0879\, r_s)/(0.0152 + 3.0426\, r_s + r_s^2)$, where $r_s \sim 1/(n^{1/3}a_x)$. We use this expression to determine the EHP density from the low-energy emission edge of the time-resolved spectra shown in Figure 2b. On a logarithmic scale, one can clearly see the low-energy edge of each of the PL spectra. Measuring the BGR as the shift from the lower edge of the exciton emission line from the nanowire (see the 2.40 ns spectrum in Figure 2b), we can see that the BGR at the low-energy edge of the 150 ps spectrum is ~40 meV, which corresponds to an EHP density of 3×10^{19} cm^{-3}. The sum of the electron and hole Fermi energies for such a density should be $E_{Fe} + E_{Fh} = 380$ meV, which is not accessible through our measurements. However, by 600 ps after the laser pulse, the BGR is now 30 meV (see left-facing arrow at bottom of graph), which corresponds to a density of 1×10^{19} cm^{-3}. The corresponding Fermi energy is 190 meV (see right-facing arrow at bottom of graph), which corresponds to the upper edge of the PL spectrum. Finally, the 1500 ps spectrum shows a BGR of 27 meV, which corresponds to a density of 6×10^{18} cm^{-3} and a Fermi energy of 140 meV. Note that the Fermi energies measured relative to the bottom of the band in each case correspond well to the upper edge of the corresponding PL spectrum. This suggests that the BGR and Fermi energies are consistent with a single density for the EHP at a particular time after the laser pulse.

The recombination lifetimes for both wire A and B are plotted as a function of emission energy as the solid symbols in Figure 4. We obtain these lifetimes by fitting the natural log of the intensity as a function of time, seen in Figure 3, to a straight line in order to extract a recombination time

for each energy. For both wires, time-resolved spectra selected at just after the laser pulse (300 ps, blue solid lines in Figure 4) and at late times after the laser pulse (2.4 ns, red solid lines, Figure 4) are displayed. The responses of wire A and wire B are similar, with large intensities at higher energies at early times moving to large intensities near the exciton energy by 2.4 ns. Relatively short recombination times are seen at high energies because of the decreasing Fermi energy as the electron−hole density decreases. Similarly, short recombination times are seen at low energies (below the exciton emission line) because of the density-dependent BGR. The lifetimes on both the high- and low-energy sides increase as the emission energy approaches the exciton emission line. The maximum lifetime is seen to occur at energies just below the exciton emission line, which corresponds to the sharp PL emission observed in the high-quality epilayer (black solid line at 1.418 eV).

This indicates that the ground state of the InP nanowire emission coincides with bulk InP exciton emission energy. Indeed, the line width measured at late times (low exciton densities) is only 20 meV. The broad width and the shift to higher energy observed in the time-integrated spectra of Figure 1d results from averaging over all energies and densities implicit in time-averaged data acquisition. The InP nanowire ground-state excitonic emission, because of its relative insensitivity to surface states, has a long lifetime, 0.52−1.1 ns, comparable to the measured InP epilayer recombination lifetime (1.7 ns, not shown), and nearly 2 orders of magnitude longer than lifetimes observed in GaAs or CdS semiconductor nanowires.[14−18] This is a remarkable result, considering that at low temperature, an exciton should diffuse laterally through the nanowire more than 1 μm during a 1 ns lifetime ($\sqrt{D\tau}$), an order of magnitude larger than the nanowire diameter.[28] Moreover, because there should be significant Fermi pressures involved with the degenerate plasma, the transport of the electron hole plasma should be even more striking. The photoexcited carriers should therefore scatter many times off the walls of the NW before recombination. Assuming that the observed lifetimes are determined by nonradiative surface recombination, we find that surface recombination velocity in these nanowires of diameter $d = 80$ nm and $\tau_{NR} = 1$ ns to be $S = d/2\tau_{NR} \approx 4000$ cm/s.

In summary, we have studied exciton dynamics and recombination in single InP nanowires. Both the energy-dependent PL decays and the time-dependent spectral evolution of PL spectra of single InP nanowires indicate that the nanowires experience continuum state filling and significant band gap renormalization at early times after pulsed excitation, with subsequent relaxation to the ground excitonic states. We have found that low surface recombination lifetime observed in bulk InP is also characteristic of high-quality InP nanowires, leading to excitonic lifetimes similar to those in the bulk. These high-quality InP nanowires display a higher quantum efficiency compared to other types of semiconductor nanowires (e.g., CdS, GaAs), thus making them attractive candidates for nanophotonic device applications.

Acknowledgment. The U.S. authors gratefully acknowledge the University of Cincinnati and the Institute for Nanoscale Science and Technology and the National Science Foundation through grants EEC/NUE 0532495 and ECCS 0701703. The Australian authors gratefully acknowledge financial support from the Australian Research Council for this work. The Korean author acknowledges financial support from KOSEF.

References

(1) Patolsky, F.; Zheng, G.; Lieber, C. M. *Anal. Chem.* **2006**, *78*, 4260−4269.
(2) Jie, X.; Wei, L.; Yongjie, H.; Yue, W.; Hao, Y.; Lieber, C. M. *Nature* **2006**, *441*, 489−493.
(3) Bryllert, T.; Wernersson, L. E.; Lowgren, T.; Samuelson, L. *Nanotechnology* **2006**, *17*, S227−S230.
(4) Huang, Y.; Duan, X. F.; Lieber, C. M. *Small* **2005**, *1*, 142−147.
(5) Greytak, A. B.; Barrelet, C. J.; Li, Y.; Lieber, C. M. *Appl. Phys. Lett.* **2005**, *87*, 151103-1−151103-3.
(6) Fasth, C.; Fuhrer, A.; Bjork, M. T.; Samuelson, L. *Nano Lett.* **2005**, *5*, 1487−1490.
(7) Agarwal, R.; Barrelet, C. J.; Lieber, C. M. *Nano Lett.* **2005**, *5*, 917−920.
(8) Samuelson, L.; Thelander, C.; Bjork, M. T.; Borgstrom, M.; Deppert, K.; Dick, K. A.; Hansen, A. E.; Martensson, T.; Panev, N.; Persson, A. I.; Seifert, W.; Skold, N.; Larsson, M. W.; Wallenberg, L. R. *Physica E* **2004**, *25*, 313−318.
(9) Samuelson, L.; Bjork, M. T.; Deppert, K.; Larsson, M.; Ohlsson, B. J.; Panev, N.; Persson, A. I.; Skold, N.; Thelander, C.; Wallenberg, L. R. *Physica E.* **2004**, *21*, 560−567.
(10) Patolsky, F.; Zheng, G.; Hayden, O.; Lakadamyali, M.; Zhuang, X.; Lieber, C. M. *Proc. Natl. Acad. Sci. U.S.A.* **2004**, *101*, 14017−14022.
(11) Barrelet, C. J.; Greytak, A. B.; Lieber, C. M. *Chem. Abstr.* **2005**, *229*, U717−U717.
(12) Fang, Q.; Yat, L.; Gradecak, S.; Wang, D.; Barrelet, C. J.; Lieber, C. M. *Nano Lett.* **2004**, *4*, 1975−1979.
(13) Barrelet, C. J.; Greytak, A. B.; Lieber, C. M. *Nano Lett.* **2004**, *4*, 1981−1985.
(14) Hoang, T. B.; Titova, L. V.; Yarrison-Rice, J. M.; Jackson, H. E.; Govorov, A. O.; Kim, Y.; Joyce, H. J.; Tan, H. H.; Jagadish, C.; Smith, L. M. *Nano Lett.* **2007**, *7*, 588−595.
(15) Titova, L. V.; Hoang, T. B.; Jackson, H. E.; Smith, L. M.; Yarrison-Rice, J. M.; Lensch, J. L.; Lauhon, L. J. *Appl. Phys. Lett.* **2006**, *89*, 053119-1−053119-3.
(16) Titova, L. V.; Hoang, T. B.; Jackson, H. E.; Smith, L. M.; Yarrison-Rice, J. M.; Kim, Y.; Joyce, H. J.; Tan, H. H.; Jagadish, C. *Appl. Phys. Lett.* **2006**, *89*, 173126-1−173126-3.
(17) Smith, L. M.; Hoang, T. B.; Titova, L. V.; Jackson, H. E.; Yarrison-Rice, J. M.; Lensch, J. L.; Lauhon, L. J.; Kim, Y.; Joyce, H. J.; Jagadish, C. *AIP Conf. Proc.* **2007**, *893*, 869−870.
(18) Hoang, T. B.; Titova, L. V.; Yarrison-Rice, J. M.; Jackson, H. E.; Smith, L. M.; Kim, Y.; Joyce, H. J.; Jagadish, C. *Nanotechnology, 2006.* IEEE-NANO 2006. Sixth IEEE Conference on Volume 1; June 17−20, 2006; pp 116−118.
(19) Mattila, M.; Hakkarainen, T.; Lipsanen, H.; Jiang, H.; Kauppinen, E. I. *Appl. Phys. Lett.* **2007**, *90*, 33101−1−3.
(20) Rosenwaks, Y.; Shapira, Y.; Huppert, D. *Phys. Rev. B* **1992**, *45*, 9108−9119.
(21) Casey, H. C., Jr.; Buehler, E. *Appl. Phys. Lett.* **1977**, *30*, 247−249.
(22) Lloyd-Hughes, J.; Merchant, S. K. E.; Fu, L.; Tan, H. H.; Jagadish, C.; Castro-Camus, E.; Johnston, M. B. *Appl. Phys. Lett.* **2006**, *89*, 232102-1−232102-3.
(23) Nelson, R. J.; Sobers, R. G. *J. Appl. Phys.* **1978**, *49*, 6103−6108.
(24) Parkinson, P.; Lloyd-Hughes, J.; Gao, Q.; Tan, H. H.; Jagadish, C.; Johnston, M. B.; Herz, L. M. *Nano Lett.* **2007**, *7*, 2162−2165.
(25) Mathieu, H.; Chen, Y.; Camassel, J.; Allegre, J. *Phys. Rev.w B* **1985**, *32*, 4042−4051.
(26) Haug, H.; Schmitt-Rink, S. *Progr. Quantum Electron.* **1984**, *9*, 3−100.
(27) Vashishta, P.; Kalia, R. K. *Phys. Rev. B* **1982**, *25*, 6492−6495.
(28) From the Einstein relation, $D = \mu kT$, where $\mu = 1000$ cm^2/Vs appropriate for high purity and low density p-type InP.

NL071733L